

A Numerical Study on Asphalt Layer Location in a Slab Track System for High-Speed Railways

M. Fang¹, D. Park², J.L. Singuranayo¹ and J.G. Rose³

¹School of Civil Engineering and Architecture

Wuhan University of Technology, Wuhan, China

²Department of Civil Engineering, Kunsan National University

Miryong-dong, Kunsan, Jeonbuk, 54150, South Korea

³Department of Civil Engineering, University of Kentucky
Lexington, United States of America

Abstract

This paper presents a quick but effective selection of the potential location for an asphalt layer implementation in a slab track system via three-dimensional numerical analysis. Based on the finite element method (FEM), one reference model with a traditional slab track (S0) and four proposed models, with an asphalt layer in different locations of slab track (S1, S2, S3, and S4), were established, followed by the reasonability verification using test data from literature. During the modelling, the bottom and the top of graded crushed stone, and the bottom of cement base, as well as the cement slab, were replaced by a certain thickness of dense and coarse asphalt mixture, respectively. The vertical acceleration and the deflection on the top of the improved subgrade layer, as well as the transversal and longitudinal tensile strain on the bottom of the asphalt layer, were the recommended mechanical parameters for structural evaluation. The results showed that the top of crushed stone replaced by the asphalt layer (S2) is the recommended solution of the asphalt layer installed in the slab track system. Meanwhile, the slab track directly installed on the asphalt layer (S4) is also a good direction for future research on asphalt slab tracks. An aggregate gradation with NMA_S = 25 mm has also been recommended in this research.

Keywords: high-speed railways, asphalt concrete, substructure, ballastless trackbed, slab track, finite element method, numerical analysis.

1 Introduction

In the last ten years, there has been a rapid incremental usage of ballastless trackbed, such as the slab track in China's high-speed railway network [1]. Conventional slab track, containing a Portland cement concrete (PCC) slab, has inherent properties of high stiffness and brittleness, high noise, and high vibration levels. Importantly, slab, working together with a PCC base directly installed on a subgrade surface, can be poorly adaptable to soil subgrades, which can increase maintenance efforts and the cost of the trackbed. Different from PCC, an asphalt mixture has a better performance,

such as considerable flexibility, reasonable stiffness with adequate strength to resist deformations, good resistance to water, and is easy to handle during construction. As a result of these important material attributes, asphalt material is widely used in highway pavement, as well as hydraulic engineering. As a matter of fact, asphalt mixture is also an important material option for railway substructures. The related applications can be found in literatures [2-8], which indicates that in the past few decades asphalt trackbeds were quite commonly used in Japan and several western European countries for high-speed railway construction, and in the United States for track rehabilitation and maintenance. Moreover, the literature reviews also revealed that the asphalt layer used in traditional ballasted trackbeds is more popular than that used in ballastless trackbeds, such as ATD and GETRACK developed in Germany.

According to the review, railway asphalt concrete substructure (RACS) can be summarized into four types [9]. (i) Pouring liquid-asphalt trackbeds (PLT), trackbed with liquid-asphalt treated for conventional ballast in usual to consolidate granular ballast; (ii) Waterproofing asphalt trackbeds (WAT), trackbed with dense asphalt concrete paved on both shoulder of tracks, which is not real railway substructure, strictly speaking; (iii) Isolating asphalt trackbed (IAT), trackbed with bearing layer of dense asphalt concrete constructed between the top layer of subgrade and the ballast or PCC slab base and, (iv) Direct-supporting asphalt trackbed (DAT), trackbed with asphalt concrete placed on the top of the ballast or subgrade layer to support sleepers or rails, directly. The schematic of four types of trackbed are shown in Figure 1.

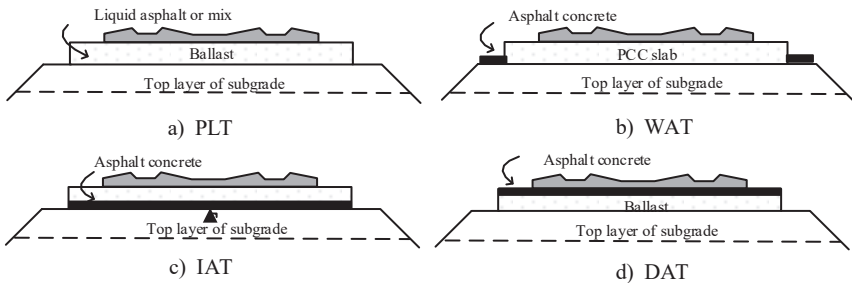


Figure 1: Classification of RACS

It is noticed that the asphalt layer, only located in IAT and DAT, can be defined as bearing layers whether used in ballasted or ballastless trackbeds. Slab track is one of the most common types of ballastless trackbed. Slab tracks can still be taken as a layered system. In this system, the basic assumptions are similar to ballasted trackbed or a highway pavement structure [9]. Compared with previous research on the recommended location of the asphalt layer placed in conventional ballasted trackbeds [10], the optimum location for the asphalt layer in the slab trackbeds should also be analyzed according to the same theory and parameters for dynamic finite element method (FEM) modelling. As a result of the high cost and complexity of laboratory tests or in-track tests, this numerical analysis is quite appropriate and necessary prior to further study.

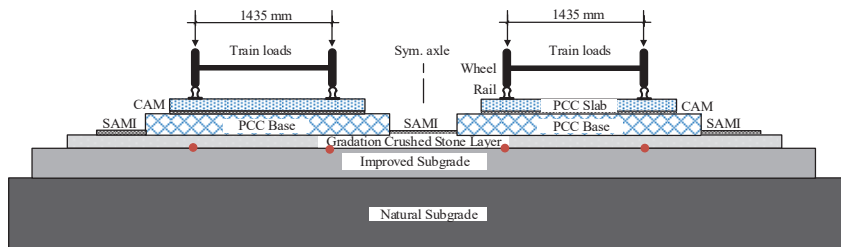
In this research, five models were established using a FEM program, one reference model with conventional slab track (Mode S0), and four models of slab substructures with different asphalt layer locations, in order to numerically select the best location of the sub-track asphalt layer for the slab trackbeds in high-speed rails. During the modelling, on the basis of Model S0, the bottom and the top of the graded crushed stone layer and the bottom of the PCC base, as well as the PCC slab, were replaced by a certain thickness of asphalt mixture, named as Models S1, S2, S3, and S4, respectively. This paper presents a quick but effective analysis of numerical determination of the optimum location of the substructure asphalt layer for ballastless trackbeds in high-speed railways. During the analysis, taking the ordinary design method of conventional highway pavement as a reference, the vertical acceleration and deformation (deflection) are applied on top of the improved subgrade layer, as well as the horizontal (transversal and longitudinal) tensile strains on the bottom of each asphalt layer as the mechanical susceptibility parameters to select the recommended type of asphalt slab trackbed.

Therefore, the main objective of this research is to provide a potential solution on the layer location of the sub-track asphalt pavement for the railway slab track system in high-speed railway lines. In addition, the findings can also, hopefully, give direction to the research on asphalt trackbed for both laboratory tests and field tests.

2 Numerical modelling

2.1 Variables consideration

The full cross-section sketch of the traditional slab trackbed Model S0 (without asphalt layer), as shown in Figure 2, was taken as the reference structural model for numerical analysis of RACS. For high-speed railways, the requirements of stiffness and strength for the slab track are much higher than that of conventional ballasted trackbed. Because it is a type of bearing layer, especially highly strict requirements of vertical displacement of substructures in post-construction are required. For example, the concept of Zero Subsidence in post-construction is taken as the settlement control for ballastless track on the soil subgrade in China [1, 9]. Fortunately, the applied asphalt mix is covered and constrained by the sub-track system, which performs a relatively isolated environment for structural stability and is totally dissimilar to that used in highway pavement designs [7].



Note: SAMI = Surface Asphalt Mix Impermeable; PCC = Portland Cement Concrete; CAM = Cement Asphalt Mortar
 ● = Data extracted points for acceleration and deflection

Figure 2: Cross-section sketch of slab track substructure (Model S0)

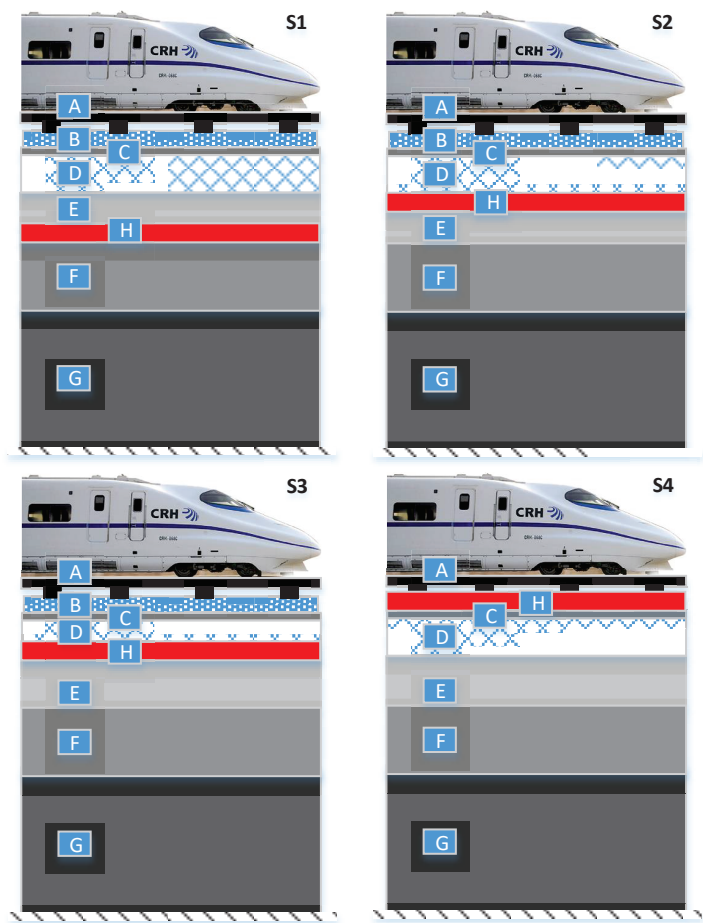
In order to analyze the optimum location of the asphalt layer in the slab track system, the substructure influenced by dynamic train loads were divided by six layers, top/middle/bottom graded crushed stone layer, top/bottom PCC base/ PCC slab layer, respectively. From the view on construction unity and materials consistency, the middle of the crushed stone layer cannot be replaced by an asphalt mixture. Moreover, if the top layer of the PCC base is replaced by an asphalt layer, the vertical stiffness of the substructure will be matched as discontinuous, and the corresponding dynamic load-spreading route will be very complicated and unreasonable. Consequently, the possible locations of the asphalt layer are at four potential positions, in which the corresponding Models S1, S2, S3, and S4 are named as the representative models for the asphalt substructures with the bottom of the crushed stone layer, the top of crushed stone layer, the bottom of the PCC base, and the PCC slab, respectively. In order to minimize the effect of the thickness of the asphalt layer on the modelling results, the same thickness of 15 cm was considered for all four asphalt trackbed models. However, for Model S4 the thickness of the asphalt layer uses 19 cm, because the total thickness of the slab is 19 cm. In addition, the cement asphalt mortar (CAM), with the function of buffering and adjusting between slab and base, did not refer to the sensitivity analysis in this FEM calculation for consideration of simplicity. Meanwhile, it is noticed that CAM has been replaced by self-compaction cement concrete in the latest development of the slab track, CRTS-III, in China.

Therefore, there are two main issues in FEM processing. One is to conduct the verification on vital responses induced by dynamic train loads for S0 with appropriate parameters. Another one is to numerically determine the optimum asphalt layer in the slab track by comparing the responses from S0 with those from four asphalt slab track structures, S1, S2, S3, S4, respectively. The sketch of the proposed sub-track asphalt layers in the longitudinal direction are shown in Figure 3.

2.2 Geometric modelling

The sub-structural components of the slab trackbed model contains rails, pads, fastener, precast PCC slab, CAM (or self-compaction concrete), PCC base, graded crushed stone layer, improved subgrade layer, and natural subgrade body (foundation soil) in vertical direction from top to bottom. All solid elements are used, considering only the bearing layers during analysis. In the longitudinal direction, there was 15 m with three slabs modelled in order to minimize the influence of the calculation results by boundary constraints. For considering reasonable simplicity, the convex column for the constraint function is not performed for analysis, and the related FEM models as considered as a continuous structure in the longitudinal direction. The calculation area on the models for data extracting and analyzing was located in the middle of 5 m long model. For the track supporting layers, the width and thickness of the slab is 2,400 mm and 190 mm, respectively; the width and height of CAM is 2,400 mm and 50 mm, respectively; the width and thickness of the base is 2,800 mm and 300 mm, respectively. In order to avoid dealing with the complicated dynamic artificial boundary, the full cross section was modelled in transversal direction for double lines. For the rails modelling, the length of the non-bolt rails with 60 kg/m and 100 m were fixed. Solid elements are used, and no curve boundary is applied for the rail cross-section to simplify it for easy meshing with the following geometric parameters: width

of railhead $b = 73$ mm, height of railhead $h = 48.5$ mm, rail waist $t = 16.5$ mm, rail height $H = 176$ mm, and rail width $B = 150$ mm.



Icons:









- | | |
|---|---|
|  A Rail |  E Gradation Crushed Stone Layer |
|  B PCC Slab |  F Improved Subgrade Layer |
|  C Cement Asphalt Mortar (CAM) |  G Natural Foundation |
|  D PCC Base |  H Asphalt Layer |

Figure 3: Longitudinal profiles of four asphalt slab track models

The layer of the surface asphalt mix impermeable (SAMI, shown in Figure 2 above) was not considered for dynamic analysis modelling as it only concerns the waterproofing function. The top and bottom layer's subgrade were 0.4 m and 2.3 m thick, respectively, and the thickness of the filling subgrade was 5 m. The width of the top subgrade was 13.5 m, and the width of the bottom subgrade layer was 16.0 m, considering design slope. The width of the filled soil subgrade was 26.5 m. All of the element types in finite element modelling were solid. The materials properties for the calculation are listed in Table 1 [9].

Part	Density/ kg/m ³	Resilient Modulus/Pa	Poisson's ratio	Damping coefficient	Materials
Rails	7830	2.06×10^{11}	0.3	0.015	Steel
PCC Slab	2450	3.65×10^{10}	0.2	0.03	C60 Concrete
CAM	2050	4×10^8	0.2	0.035	Emulsified Asphalt, Cement, Sands
PCC Base	2300	3.4×10^{10}	0.2	0.03	C40 Concrete
Gradation Crushed Stone Layer (Top of Subgrade)	2200	1.5×10^8	0.25	0.045	Unbound Gradated Aggregates
Improved Subgrade Layer	2000	0.6×10^8	0.25	0.039	Improved Soils
Natural Foundation	1800	0.5×10^8	0.33	0.035	Unimproved Soils

Table 1: Materials properties used in calculation

2.3 Finite element modelling

All materials, including rails, fastener system, PCC slab, CAM, PCC base, and subgrade body are used as linear elastic constitution, which is related to parameters such as mass, density, elastic modulus, Poisson's ratio, and damping coefficient. According to the related literatures [10, 11], the Springs-Dashpots elements used for the connection were between the rails and slabs. The vertical stiffness and damping are 70 kN/mm and 60 kN•s/m, respectively, and the transversal stiffness and damping are 30 kN/mm and 50 kN•s/m, respectively. For the asphalt layer, the elastic modulus and Poisson's ratio are used with 4000 MPa and 0.35, respectively, and the density is 2400 kg/m³. The other parameters are the same with the reference structure under 200 km/h dynamic loads and the same boundary conditions. The traditional model for S2 after meshing is shown in Figure 4, and the other four models are similar to S2.

The bottom of each model was constrained in all six degrees of freedom. A symmetric boundary condition was applied for two cut sections along the rail direction. There was no other boundary constraints in the modelling. For the consideration of reasonable simplicity, a continuous condition was applied for all interfaces. The mesh of the models was generated by an eight-node inducing integrated element (C3D8R) arising from its higher accuracy with lower computational time [12].

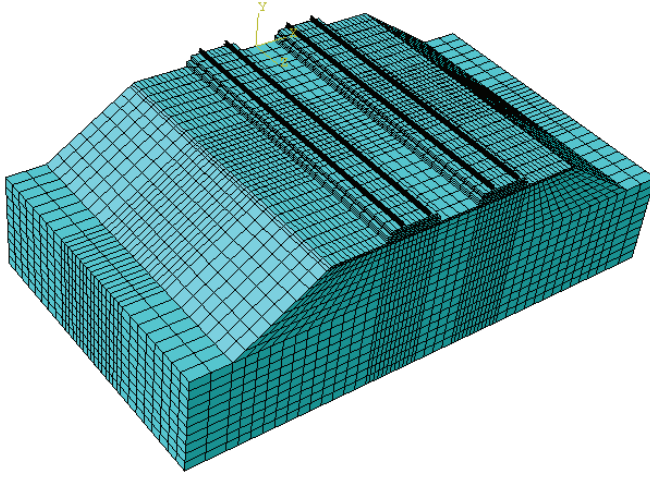


Figure 4: Finite element model after meshing

2.4 Modelling of train load

The ellipse contact area of wheel-rail loads was simplified as a rectangle, and the exciting load model was adopted to simulate the dynamic loads of the train [13], and each track line was subjected to a set of wheel loads. The trainload expression is used as the equation below:

$$F(t) = P_0 + P_1 \sin \omega_1 t + P_2 \sin \omega_2 t + P_3 \sin \omega_3 t \quad (2)$$

in which, P_0 = the unilateral static wheel load; P_1 , P_2 , P_3 = the vibration loads computed by three control conditions, train stationary (I), dynamic additional load (II) and corrugations (III), respectively. If the unsprung weight of the train is M_0 , the related amplitude of vibration load is:

$$P_i = M_0 \alpha_i \omega_i^2 \quad (3)$$

where, α_i and ω_i are the vector height and the circular frequency of vibration wavelength corresponding to the above three control conditions, respectively. The expression of which is the following equation:

$$\omega = 2\pi v / L_i \quad (4)$$

where, v is the train speed in km/hr; L_i is the corresponding vibration wavelength in m. Because the dynamic additional load (II) and the corrugation effect (III) are not the focus of this research, the trainload in this modelling can be modified as follows:

$$F(t) = P_0 + P_1 \sin \omega t \quad (5)$$

$$P(t) = F(t) / A = (P_0 + P_1 \sin \omega t) / A \quad (6)$$

where, A = the loading area. From the data of common high-speed trains [9], when $P_0=125$ kN, $M_0=750$ kg, $a=0.4$ mm, $A=940$ mm², $L=2$ m. In this paper, the reference velocity is 200 km/h which is the minimum speed for high-speed railways. According to the equations above, If $v = 200$ km/h, then $\omega = 174.5$ Hz, $P_1=9.1$ kN. The time history curve of train loads at speed of 200 km/h is shown in Figure 5.

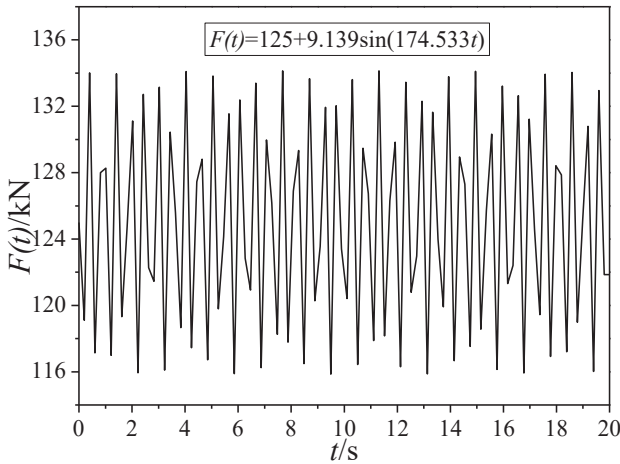


Figure 5: Time-history curve of train loads (200 km/h)

3 Results and Analysis

3.1 Verification for reference Model S0

For the reference Model S0, the amplitude of the vertical acceleration on the top of the subgrade layer is in the range from -23 m/s² to $+19$ m/s²; most of the calculated values are still in the range from -5 m/s² to $+5$ m/s², which covers the verification values 0.01 - 2.587 m/s² from literature [14]. The corresponding vertical deformation of S0 is in the range from 0.5 mm to 1.8 mm, which is in the amplitude of the verification data, 0.003 - 0.77 mm [14]. The calculated vertical stress amplitude on the top of the subgrade layer ranges from about 12 kPa to 25 kPa, which contains the average value 14.5 kPa presented in the literature [15], but which is slightly lower

than the simulated values 0.036–0.096 MPa calculated in another literature [16]. Considering the differences of conditions in this numerical calculation, compared to the verification data, Model S0 is reasonable to take as the reference structure in research. Therefore, four other models, S1, S2, S3, and S4, are also available for analysis arising from the modelling developed from reference model S0.

3.2 Vertical Acceleration

As shown in Figure 6, Model S2 reduces the vertical accelerations among four asphalt slab tracks compared with the results from reference Model S0.

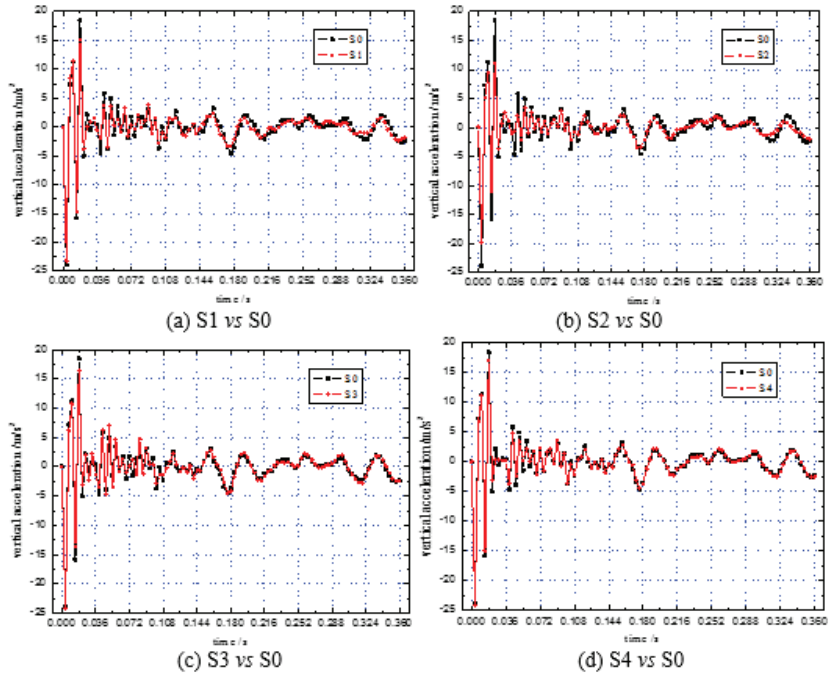


Figure 6: Comparison of vertical accelerations time-history curves on the top of improved subgrade layer

Specifically, the acceleration on the top of Model S3's subgrade layer is greater than that of S0, particularly during the time history from 0.036 s to 0.072 s, where the acceleration rate of decay is slower. For Model S4, the decay rate of acceleration is similar to that of S0, and only the peak value is slightly smaller than that of S0. The peak values of the vertical acceleration of S1 are also lower but the amplitude is less than that of Model S2, even though the Model S1 can also be taken as one of the optimal options. For Model S2, the rate of decay is changed quickly, and, also the

range of peak values decreased from about $-24/+18 \text{ m/s}^2$ to about $-19/+12 \text{ m/s}^2$ compared to that of S0. From the calculated results, Model S1 and Model S2 are the two appropriate options for optimal structures and Model S2 is the best option.

3.3 Vertical displacement

The time history curves of vertical displacement on the top of the improved subgrade layer of reference Model S0 and four asphalt track Models, S1, S2, S3, and S4, were extracted, as shown in Figure 7.

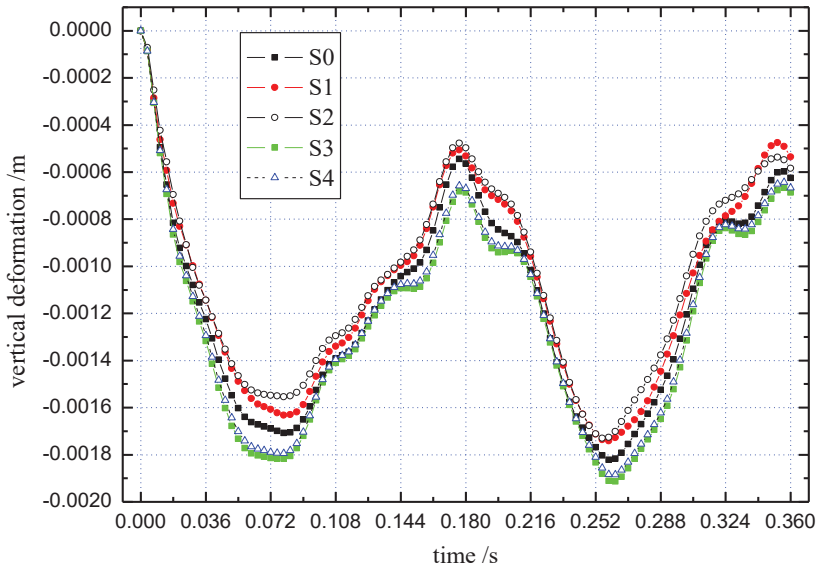


Figure 7: Time-history curves of five track models for vertical displacements

According to the comparative analysis, the peak values of deflection of S3 and S4 are greater than the other three structures, S0, S1, and S2, and the low value is about 1.8-1.9 mm and the high is about 0.7 mm during the time history. The values are about 0.67-0.69 mm at the end of the calculation period. The values of vertical deformation calculated from S1 and S2 are less than that of reference Model S0, in which the low peak values of S1 and S2 are about 1.55-1.63 mm, and that of S0 is about 1.71 mm, which is 5%-9% less than that of S1 and S2. The high peak values, Model S1 and Model S2, are about 0.48-0.51 mm, and that of S0 is about 0.54 mm, less than that of S1 and S2 by 6%-11%. In addition, at the end of the calculation period the vertical deformation on the top of the improved subgrade layer of five modelling structures, Model S0 to Model S4, are about 0.624 mm, 0.535 mm, 0.584 mm, 0.687 mm and 0.667 mm, and in general the deflection of Model S2 is less than that of Model S1.

The vertical deformation of the improved subgrade layer, such as the graded and crushed stone layer, shows that Model S1 and Model S2 are more appropriate types of asphalt slab track than Model S3 and Model S4, in which the Model S2 with slightly less deformation can be taken as the best option.

3.4 Horizontal strains

The horizontal strains, including in transversal and longitudinal direction as well as the maximum horizontal tensile strains at the bottom of the asphalt layer of the four slab trackbeds, are compared, as shown in Figures 8(a), 8(b), and 8(c), respectively. The results show that the maximum horizontal strain in longitudinal direction for the bottom of the railway asphalt layer is about $-24.371 \mu\epsilon$ (compression strain), which indicates the slab would be in compression if replaced by the asphalt layer. As this is similar to the other materials used in civil engineering, the asphalt concrete has the advantage performance on compression while not tensile. Therefore, in terms of the calculation results of longitudinal compression strain, Model S4 can be taken as asphalt railway trackbeds.

For Model S1, the maximum horizontal tensile strain is about $21.049 \mu\epsilon$, which is the highest among the four asphalt trackbeds structures, and the maximum longitudinal tensile strain is $39.713 \mu\epsilon$, which is similar to those of Model S2 and Model S4. However, the horizontal strain of the transversal tensile strain in Model S1 has obviously fluctuated with the amplitude from -8 to $20 \mu\epsilon$, which will decrease the fatigue life of the asphalt mix. Therefore, S1 is not the appropriate asphalt trackbed in terms of transversal strain of the asphalt layer. In addition, the strain level at the bottom of the asphalt layer for Model S2 and Model S3 are similar to, though slightly greater than, Model S4. From the theoretical analysis on horizontal strain, direct-supporting asphalt trackbed (DAT), Model S4, can perform at a good capacity for fatigue resistance, almost without tensile strain. However, the greater train loads transferred from the slab can have a high risk on the vertical deformation stability of the asphalt layer, which should have further study, especially to conduct laboratory tests, or even field tests.

Based on transversal tensile strain, both Model S2 and S4 can be considered as forms of asphalt slab trackbed, in which the asphalt layer located in Model S4 can be taken as a better bearing layer for minimizing compression stresses, however, it is also subjected to dynamic train loads transferred from the fastener system which can cause quite complicated mechanical behaviour. Consequently, the corresponding substructure related to Model S4 still requires further research. However, it is believed that Model S4 will provide acceptable performance whether in terms of transversal strain or longitudinal strain on the bottom of the asphalt layer.

The summarized analysis of results is shown in Table 2, the Model S2 has an obvious advantage for being the best option for the asphalt ballastless trackbed. (Note: " \sqrt " means a suitable solution for optimum asphalt location in the slab track system; " \times " means it not suitable for that)

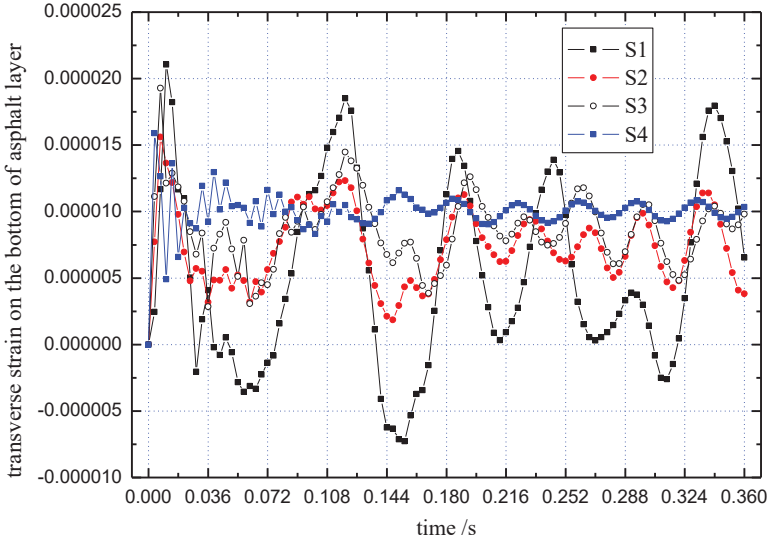


Figure 8(a):Time history curve of transversal strains at the bottom of asphalt layer

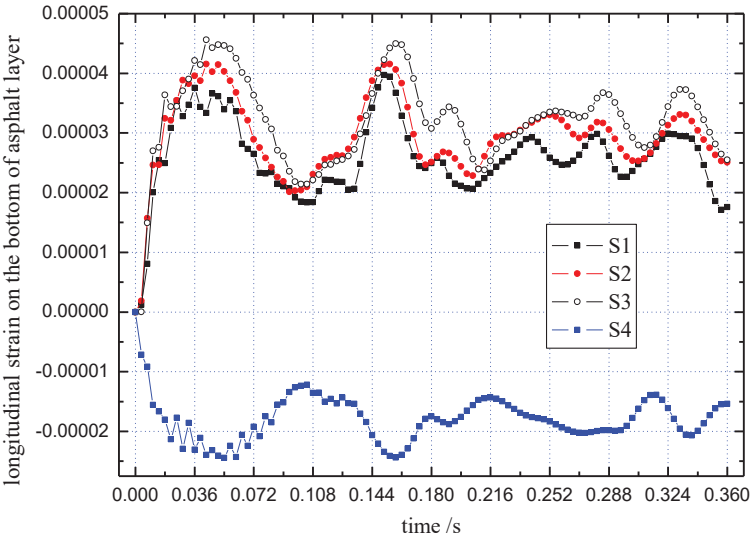


Figure 8(b): Time history curve of longitudinal strains at the bottom of asphalt layer

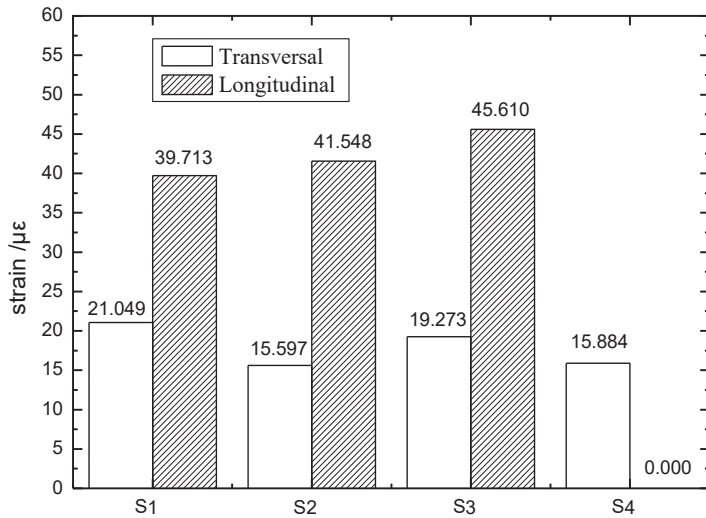


Figure 8(c): Maximum horizontal tensile strains at the bottom of asphalt layer

Options	Top of improved subgrade layer		Bottom of asphalt layer	
	Vertical acceleration	Deflection	Trans. strain	Long. Strain
S1	√	√	×	√
S2	√	√	√	√
S3	×	×	√	√
S4	×	×	√	√

Table 2: Comprehensive evaluation on different types of asphalt slab trackbeds

3.5 Test validation

In this research, the tests in the laboratory or in the field, and the economic analysis have not been conducted arising from the focus on the optimum location of the asphalt layer in the slab track system. However, several corresponding researches have been carried out already, which can be taken as the validation for this numerical research to a certain degree. The full-scale test [17] in Korea indicated that the measured tensile strains related to fatigue life at the bottom of the asphalt layer were less than a hundred micro strain ($\mu\epsilon$). The asphalt layer, therefore, can be expected to support train loads without developing major cracking during the service life of the asphalt trackbed. Permanent deformations were less than 2 mm after the whole static loading cycle was applied. As for the construction, the initial cost should be a little more than the conventional design, but from the view of life cycle cost, it will be much less than the design without asphalt installation. In addition, the asphalt layer paved on the top of the crushed stone layer can save a large amount of materials because a

certain degree thickness of the top layer of crushed stone could be replaced by the asphalt mixture. Thus, this can considerably lower the cost of construction, which can be verified in literature [18]. However, more research, such as a physical model, and even a field test directly related to this optimum asphalt location, should be strongly suggested to verify the rationality and economy.

In addition, according to the requirements of bearing capacity for railway substructure and the authors' experience on RAM [9], the nominal maximum aggregate size (NMAS) = 25 mm is recommended for RAM and the aggregate gradation can be used, as listed in Table 3.

Sieve size/mm	Lower limit/%	Upper limit/%
37.5	100	100
26.5	90	100
19	78	95
16	67	87
13.2	56	80
9.5	42	68
4.75	29	57
2.36	19	45
1.18	14	34
0.6	10	25
0.3	5	17
0.15	3	10
0.075	1	7
<0.075	—	—

Table 3: Recommended aggregate gradation for RAM (NMAS=25mm)

4 Conclusions

By selecting the slab track system as the reference Model S0, four slab track Models (S1, S2, S3, and S4) with asphalt layer were established via the FEM program. According to the analysis on four mechanical parameters, the vertical acceleration and deflection on the top of the improved subgrade, as well as the tensile strain on the bottom of the asphalt layer, and the recommended location of the asphalt layer in railway slab track was selected based on modelling analysis. From this numerical analysis, the following conclusions can be drawn.

(i) S0 has been effectively validated as the reference model for numerical analyses by comparing three parameters: i) the amplitude of vertical acceleration, ii) the corresponding deflection, and iii) the stress on the top of the improved subgrade layer. The four models (S1 to S4) are also effective for finite element modelling based on reference Model S0. The four mechanical parameters, vertical acceleration, deflection, transversal and longitudinal strains, are reasonable to evaluate the performance of railway asphalt substructures, which can differentiate the responses of four asphalt slab tracks, as similar to asphalt pavement design. These two findings

suggest a recommended parameter system to verify the reasonability of numerical modelling on railway trackbed.

(ii) The calculated data shows that the Models S1 and S2 are more appropriate for asphalt slab track than Models S3 and S4. According to the analysis of the mechanical parameters, it can be seen that Model S2 is, relatively, a better type of asphalt slab track since it has less deformation and fluctuation of the horizontal tensile strain. In addition, the asphalt layer of Model S4 is directly subjected to dynamic train loads transferred from the fastener system, which causes complicated mechanical behaviour. However, Model S4 showed the maximum horizontal strain on the bottom of the asphalt layer is about $-24.371 \mu\epsilon$, which is beneficial for the long-term performance of the railway substructure. Slab track directly installed on the asphalt layer can save the clearance of construction and make the vertical modules distributed reasonably, which is a good direction for future research on asphalt railway trackbed,

(iii) Model S2, in which the asphalt layer is paved on the top of a graded crushed stone layer, has excellent performance whether in terms of transversal strain or longitudinal strain on the bottom of the asphalt layer, and can be taken as the optimum solution. This location is the optimum placement option for asphalt layer to slab track based on this limited numerical analysis. Importantly, dense asphalt mixture with NMA=25 mm and thickness=15cm as well as a gradation range is recommended for future research on RAM. The total thickness for the top and bottom layer of the subgrade can be decreased from the current 2.7 m to 2.3 m or less arising from the reinforcement by the asphalt mixture, which can save a lot of construction materials.

The findings in this numerical research provides a quick but effective determination on the selection of the sub-track asphalt layer for traditional ballastless track systems. However, further validation research by performing physical tests in the laboratory or in the field is strongly recommended, which is also the research perspective of asphalt trackbed used in high-speed rails. Moreover, only linear instantaneous responses with a simplified vehicle model has been established in this analysis, a more detailed modelling is also required in future to better simulate the test response. In addition, CAM in this research was not subjected to the sensitive analysis, while CAM plays an important role in the dynamic performance of the asphalt track. For the latest slab track in China, CRTS-III with self-compaction concrete has been applied instead of CAM. Therefore, the further study, with consideration of CAM or self-compaction concrete, should also be conducted in the future work. Another interesting work in future is to study the reasonable thickness of the improved subgrade to match the asphalt trackbed in the slab track system. Compared to the asphalt sub-layer in conventional ballasted track, a large amount of research needs to be carried out on the asphalt slab track system arising from the rigorous deformation control for the slab track design.

Acknowledgements

This research was supported by National Natural Science Foundation of China (No. 51308429). Meanwhile the research presented in this paper was a partial content

further developed on the framework established by author's Ph.D program, titled Structural Behaviour and Mix Design for Asphalt Concrete Substructures in High-Speed Rails. In addition, the authors appreciated the anonymous reviewer(s) for the constructive suggestions and comments.

References

- [1] He H. "Ballastless Track Shall be Developed in Great Efforts on Chinese Passenger Dedicated Lines. *Chinese Railways*", (1):11-15, 2005.
- [2] Lee S, Park D, Vo H, Dessouky, S.. Asphalt Mixture for the First Asphalt Concrete Directly Fastened Track in Korea. *Advances in Materials Science and Engineering*, 1-6, 2015, Doi: 10.1155/2015/701940.
- [3] Lee S, Lee J., Park D, Vo, H.V., "Evaluation of Asphalt Concrete Mixtures for Railway Track", *Construction and Building Materials*, 73 (30):13–18, 2014
- [4] Momoya Y., Sekine E., "Performance-based Design Method for Railway Asphalt Roadbed", *Doboku Gakkai Ronbunshuu E*, 63(4):608-619, 2007.
- [5] Lechner B., "Ballastless Tracks on Asphalt Pavements Design and Experiences in Germany", *Proceedings of the BCRA2005 - International Conference on Bearing Capacity of Roads, Railways and Airfields Conference*, Trondheim, Norway, 5-20, 2005.
- [6] Teixeira P., Lopez-Pita A., "Viability of Using Bituminous Subballast Layer on High-Speed Ballasted Tracks", *Proceedings of the BCRA2005 - International Conference on Bearing Capacity of Roads, Railways and Airfields Conference*, Trondheim, Norway, 27-29, 2005.
- [7] Rose J, Teixeira P and Veit P. International Design Practices, Applications, and Performances of Asphalt/Bituminous Railway Trackbeds, *GEORAIL 2011 - International Symposium*, Paris, France, May 19-20, 2011.
- [8] Fang M., Wu S., Park D, Chen, H, Xie, J., Simple test study on anti-freeze additives selection for railway asphalt mixture (RAM) in cold region. *Construction and Building Materials*, 154, 284-293, 2017, Doi: 10.1016/j.conbuildmat.2017.07.212
- [9] Fang M., "Structural Behavior and Mix Design for Asphalt Concrete Substructures in High-Speed Rail", *PhD Dissertation of Southwest Jiaotong University*, Chengdu, P. R. China, 2012.
- [10] Fang M., Cerdas S., Qiu Y., "Numerical Determination for Optimal Location of Sub-Track Asphalt Layer in High-Speed Rails", *Journal of Modern Transportation*, 21(2):103-110, 2013.
- [11] Lei X., Chen S., "Space Dynamic Analyses for Track Structure of High Speed Railway", *Journal of China Railway Society*, 22(5):76-80, 2000.
- [12] Hibbitt, Karlsson and Sorensen, Inc. *ABAQUS/Standard User's Manual, ABAQUS/CAE User's Manual, ABAQUS Keywords Manual, ABAQUS TheoryManual*. HKS Inc., 2010.
- [13] Jenkins H., Stephenson J., Clayton G., Morland, G.W., "The Effect of Track and Vehicle Parameters on Wheel/Rail Vertical Dynamic Forces", *Journal of Railway Engineering Society*, 3(1):.2-16, 1974.

- [14] Fan S., “Analysis on Experiment of Dynamic Response in Ballastless Track Subgrade of High-Speed Railway”, *Master Degree Thesis of Southwest Jiaotong University*, Chengdu, P. R. China, 2010.
- [15] Wei Y., Qiu Y., “Research on the Subgrade Surface Stiffness of Ballastless Track of High-Speed Railway”, *Journal of Railway Engineering Society*, 2010, (7):15-20, 2010.
- [16] Cai Z., Zhai W., Wang K., “Calculation and Assessment Analysis of the Dynamic Performance for Slab Track on Sui-Yu Railway. *China Railway Science*, 27(4):17-22, 2006.
- [17] Lee S., Choi Y., Lee H., Park, D., “Performance Evaluation of Directly Fastened Asphalt Track using a Full-Scale Test”, *Construction and Building Materials*, 113, 404-414, 2016, DOI: [10.1016/j.conbuildmat.2016.02.221](https://doi.org/10.1016/j.conbuildmat.2016.02.221)
- [18] Teixeira P., Ferreira P., Lopez Pita A., Casas, C., Bachiller, A., “The Use of Bituminous Subballast on Future High-Speed Lines in Spain: Structural Design and Economical Impact. *International Journal of Railway*, 2(1):1-7, 2009.